

Thermoelectric power of two-dimensional Pd and Pd-Au films

M. J. Burns and P. M. Chaikin

Department of Physics, University of California, Los Angeles, California 90024

(Received 18 November 1982)

We have studied the effects of two-dimensional electron localization on the temperature dependence of the resistivity and thermoelectric power of palladium and palladium-gold alloy thin films. All "metallic" ($R_{\square} < 30 \text{ k}\Omega/\square$) samples have a small material specific thermopower which tends to zero as $T \rightarrow 0$. Samples whose resistivity increases above $30\,000 \Omega/\square$ have thermopowers which increase as $T \rightarrow 0$. Thus the density of states for the electronic transport is zero at the Fermi energy for high-resistivity films.

I. INTRODUCTION

Several years ago Thouless and co-workers performed calculations which suggested that there might be a minimum metallic conductance in reduced dimensional electronic systems. This suggestion has stimulated considerable theoretical¹⁻¹³ and experimental¹⁴⁻²¹ work on electron localization in two dimensions.² The possibility of a minimum metallic conductivity is hinted at by the Ioffe-Regel rule²² which states that for metallic conduction to take place one must have $k_F L > 1$ where L is the electron mean free path and k_F is the Fermi wave number. For a two-dimensional (2D) metallic system the conductivity is

$$\sigma = (e^2/2\pi\hbar)k_F L \quad (1)$$

and conventional transport theory breaks down when $k_F L = 1$, implying a universal minimum conductivity of

$$\sigma = (e^2/2\pi\hbar) = (30\,000 \Omega/\square)^{-1}, \quad (2)$$

Scaling theories now predict that all electronic states are localized in two dimensions rather than the existence of a minimum metallic conductivity of $R_{2D}^{-1} = (30\,000 \Omega/\square)^{-1}$. Samples show a logarithmic temperature increase in resistivity for $R/\square = R_{\square} < R_{2D}$ crossing over smoothly to an exponential increase (with decreasing temperature) for $R_{\square} > R_{2D}$.³ An interacting electron picture⁴ can also give rise to the logarithmic resistivity for $R_{\square} < R_{2D}$. Resistivity measurements on thin metallic films^{14,17,19,20} and electron inversion layers^{16,18} are consistent with both scaling and interaction pictures. Magnetoresistance and Hall-effect measurements show different relative importance for the two pictures in different materials.

Resistance (and magnetoresistance) measurements

probe the carrier density and mobility but not the carrier energy distribution. The thermoelectric power (S) is an excellent probe of the carrier energy distribution about the Fermi energy (E_F). If the energy distribution falls to zero about E_F as $T \rightarrow 0$ then $S \rightarrow 0$, which is the usual case for metals as well as for variable range hopping. If S increases as $T \rightarrow 0$ then the conducting electrons transport more than thermal energy and there is evidence for the existence of an energy gap.

In this paper we present thermopower measurements on films of Pd and Pd-Au alloys which clearly indicate the opening of an energy gap as $R_{\square}(T)$ crosses above R_{2D} . A shorter study for the Pd films has been published in Ref. 20. For films with $R_{\square} < R_{2D}$ the thermopower is material specific but independent of R_{\square} and decreases with decreasing temperature. Films with $R_{\square} > R_{2D}$ show the low-temperature thermopower increasing with decreasing temperature, with the higher resistivity films showing a larger thermopower. The thermopower measurements therefore indicate that the density of states at the Fermi energy vanishes and an energy gap opens up as R_{\square} passes above R_{2D} .

II. EXPERIMENT

The samples were prepared by electron beam deposition of Marz-grade palladium and a palladium-gold alloy ingot previously prepared in an arc furnace from Marz-grade palladium and 6n gold (58% gold, 42% palladium by weight) at 0.1–1.0 Å/sec onto a glass substrate at room temperature. Pressure in the evaporator was 10^{-6} – 10^{-7} Torr during evaporation and thickness was measured with a quartz-crystal deposition controller.

Since we were unable to take electron micrographs of the actual samples used in our transport study

due to the glass slide substrate, we took electron micrographs of similarly prepared films deposited on quartz and carbon film electron microscope grids (the quartz film was ~ 500 Å on top of the carbon film grid). Figure 1 shows electron micrographs of nominal 24-Å-thick Pd and 25-Å-thick Pd-Au films deposited on a carbon film electron microscope grid. This micrograph and others of similarly prepared Pd and Pd-Au films of nominal thicknesses 18–30 Å show continuous films of fairly uniform thickness with a large number of nonpercolating cracks. The samples are therefore highly inhomogeneous on a scale of 100 Å but appear quite homogeneous on a 1- μm scale. Similar micrographs were obtained for

samples evaporated directly on the quartz-coated carbon film grids.

An electron-diffraction study shows crystalline grains of approximately 50 Å dimensions and fcc structure. The diffraction study for the Pd-Au films also indicates approximately 50-Å crystallites with fcc structure but with more disorder than similar Pd films.

In Fig. 2 we have plotted the thickness dependence of the resistivity of a palladium film at room temperature. The resistivity was monitored *in situ* during the evaporation. The film was deposited onto a glass slide at ~ 0.1 Å/sec. An electrometer first indicated an increased conductivity ($\sim 10^{-12}$

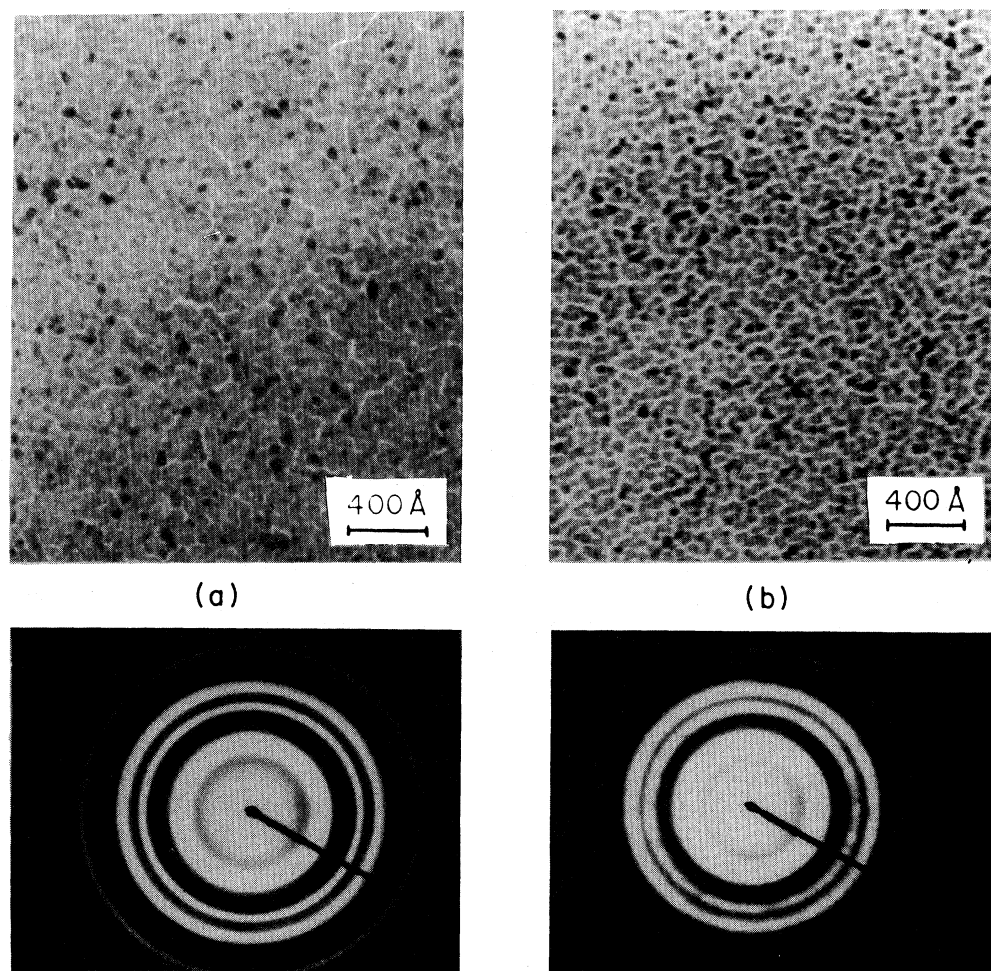


FIG. 1. Electron micrograph and electron diffraction pattern of (a) nominal 24-Å-thick palladium film, (b) nominal 25-Å-thick palladium-gold film. Both films are deposited on carbon-coated grids.

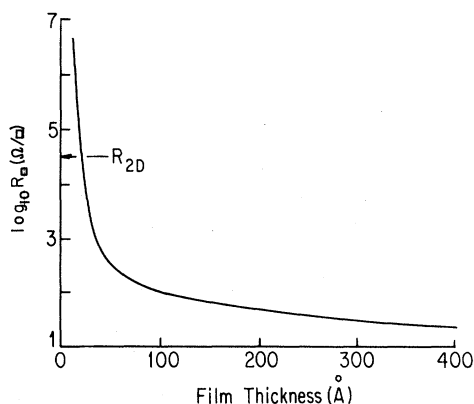


FIG. 2. Resistivity vs film thickness measured *in situ* for a palladium film deposited on glass at room temperature.

Ω^{-1}) at a nominal thickness of $\sim 4 \text{ \AA}$. The resistance then fell smoothly but rapidly and crossed the interesting value of $30 \text{ k}\Omega/\square$ at $\sim 25 \text{ \AA}$. At thicknesses greater than approximately $50\text{--}100 \text{ \AA}$ the resistivity goes as the inverse of the film thickness indicating a mean free path of about $50\text{--}100 \text{ \AA}$ at room temperature.

The experiments were performed in a sealed temperature-controlled copper sample holder placed in an exchange-gas can and submerged in liquid helium. Contact pads to the films were made with 3000 \AA of evaporated silver. The samples were mounted so that one of the silver pads rested over a copper step heat sink to which the glass slide was attached (Fig. 3). The remainder of the slide was cantilevered into the vacuum. A single-crystal quartz block with a heater attached was then glued on top of the other silver pad. Thus the heat flow was through the glass slide to the heat sink and the temperature gradient was established in the substrate supporting the thin metal films. Lead (Pb) wires were then indium soldered or silver painted to the silver pads and a $50\text{-}\mu\text{m}$ Chromel-Constantan differential thermocouple was placed in close proximity to the Pd thin-film junction to monitor the temperature difference.

The Pb sample leads and the differential thermocouple were heat sunk to the copper sample holder to avoid additional temperature gradients from the room-temperature leads. Current was supplied to the heater to establish a temperature difference of $\sim 0.3 \text{ K}$ and the voltage from the sample and differential thermocouple were plotted on an $x\text{-}y$ recorder. The current was then turned off and the gradient diminished to check for temperature drifts.

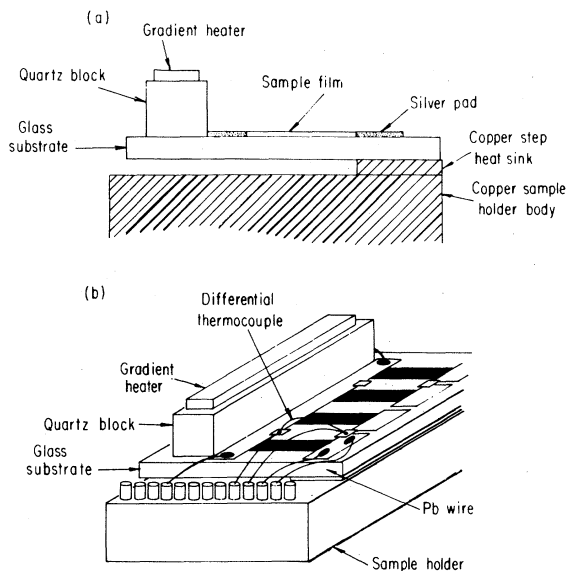


FIG. 3. Sample arrangement on copper holder; (a) cross section, (b) offset view. Sample substrate was cantilevered on step on holder with heater placed on far end. Holder was sealed in copper can which was placed in an exchange-gas can and submerged in liquid helium. All leads to samples and thermocouples were heat sunk to the sample holder to avoid additional gradients from the room-temperature leads.

The absolute accuracy of our thermopower measurement is approximately 20%.

III. EXPERIMENTAL RESULTS

In Fig. 4 we have plotted the logarithm of the resistivity as a function of the square root of the reciprocal temperature for Pd and Pd-Au samples of nominal thicknesses $18\text{--}25 \text{ \AA}$. The Pd data also appeared in Ref. 20. The resistive behavior of these films is indistinguishable from the behavior reported for quench-condensed copper and gold films.¹⁴ For resistivities greater than R_{2D} the temperature dependence is approximately an exponential with a square-root inverse power of temperature. For resistivities less than R_{2D} the temperature dependence of the resistance is considerably less and the resistivities appear flat on these plots.

In Fig. 5 we have plotted the change in resistivity divided by the square of the resistivity as a function of $\log T$. The palladium [Fig. 5(a)] films show a resistance minimum at $10\text{--}15 \text{ K}$ which proceeds to a $\log T$ dependence as the temperature is lowered and

achieves a completely logarithmic dependence for $T < 4$ K. Similarly prepared Pd films show this logarithmic behavior down to 0.1 K.¹⁹ The palladium-gold films in Fig. 5(b) display the same basic loga-

rithmic temperature-dependent resistivity as the palladium films with just a slightly lower slope. For palladium samples with $R_{\square} < 5$ k Ω and $T < 4$ K we find

$$[R_{\square}(T) - R_{\square}(10 \text{ K})] / [R_{\square}(10 \text{ K})^2] = [(2.6 \pm 0.1) \times 10^{-5} \Omega^{-1}] \log_{10}[T / (10 \text{ K})] \quad (3)$$

while for palladium-gold samples with $R_{\square} < 8$ k Ω and $T < 4$ K we find

$$[R_{\square}(T) - R_{\square}(10 \text{ K})] / [R_{\square}(10 \text{ K})^2] = [(2.3 \pm 0.1) \times 10^{-5} \Omega^{-1}] \log_{10}[T / (10 \text{ K})]. \quad (4)$$

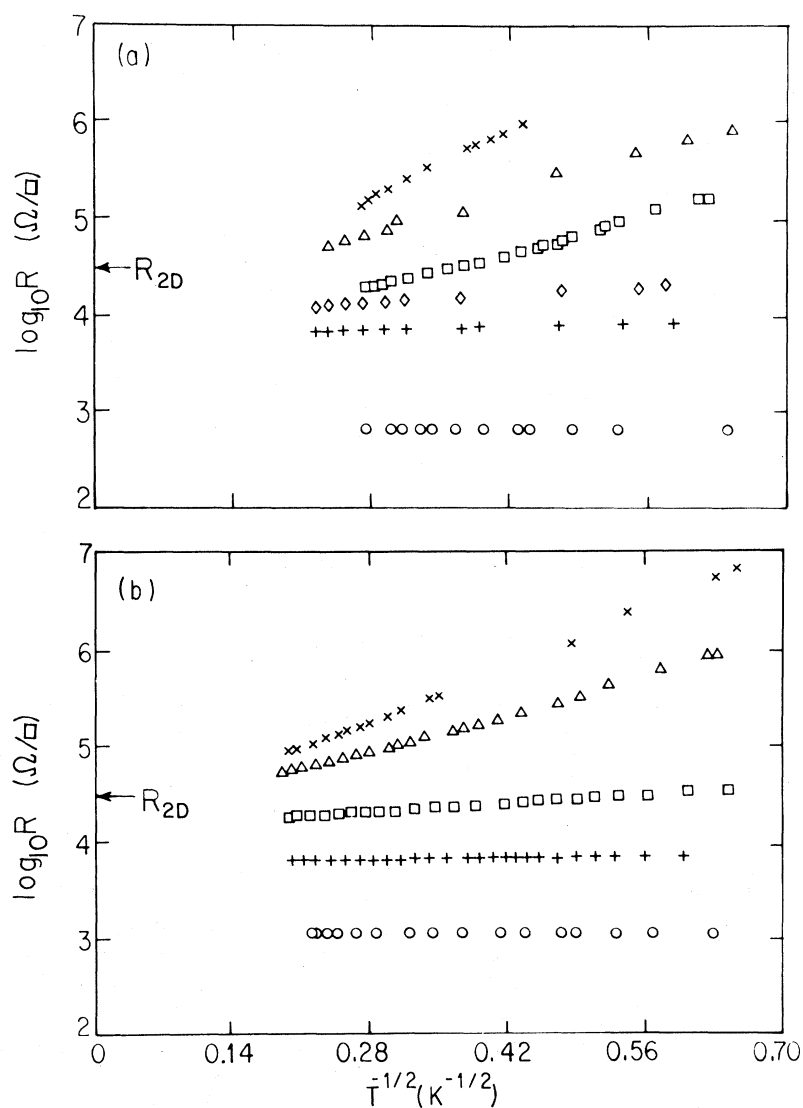


FIG. 4. Logarithm of the resistivity (in Ω/\square) as a function of reciprocal square-root temperature for (a) palladium, (b) palladium-gold films used in the thermopower study. We have used the same symbol for each film (within a material type) in all of the figures.

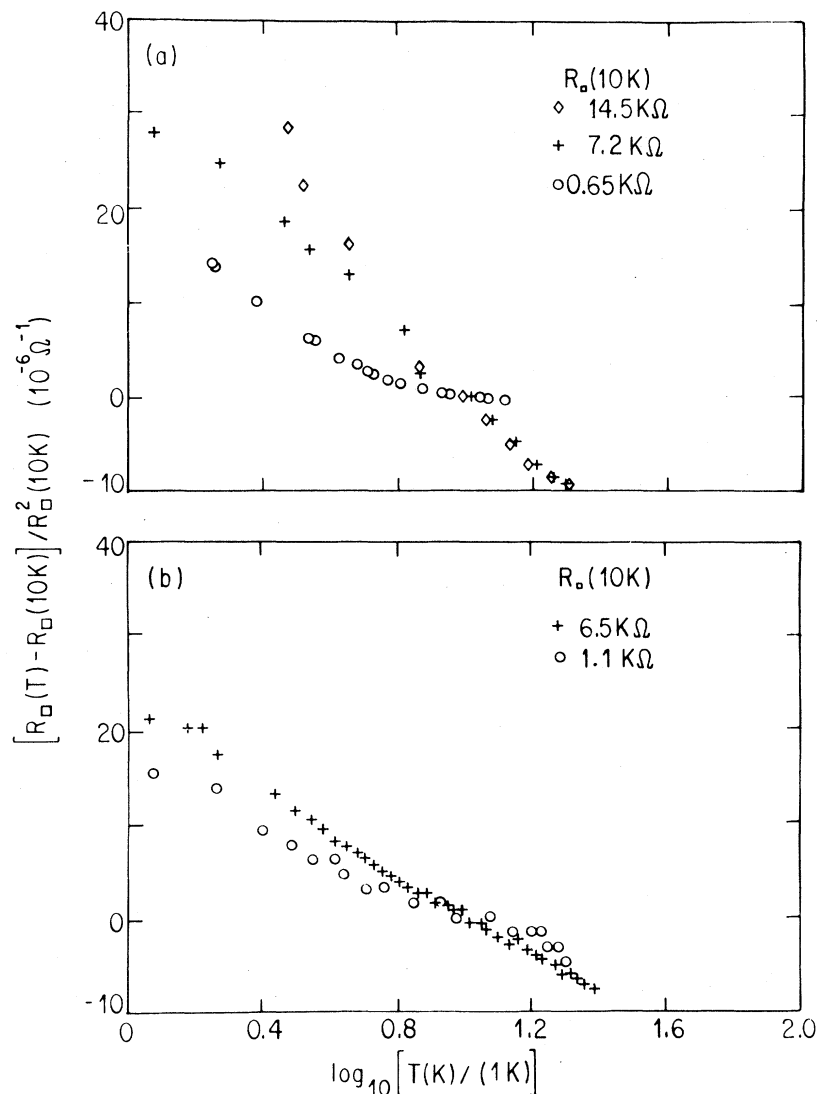


FIG. 5. Resistivity change divided by square of resistivity as a function of $\log_{10} T$ for (a) three Pd and (b) two Pd-Au film samples which show "metallic" thermopower.

These numbers are similar to what others have found for Pd-Au,¹⁵ $(2-4) \times 10^{-5} \Omega^{-1}$. We note that the values for this coefficient are close to what one expects from the "early" interaction model⁴ ($2.8 \times 10^{-5} \Omega^{-1}$) and about a factor of 2 smaller than what one expects from the early localization picture^{3,5,17} with a two-dimensional phonon density of states. They are consistent in the localization picture with an inelastic scattering mechanism with a linear temperature dependence.

For R_{\square} greater than approximately $10 k\Omega$ the low-temperature increase becomes more rapid as stronger localization and interaction effects become

important as R_{2D} is approached. The resistivity studies show that these Pd and Pd-Au films have the same behavior, at high and low R_{\square} , as thin metal films reported by other groups where only resistivity measurements were performed. Our Pd and Pd-Au films are largely indistinguishable in their temperature-dependent resistance and magnetoresistance.¹⁹ Although the thermoelectric power is of course material dependent, the low-temperature behaviors are quite similar.

The absolute thermoelectric power (corrected for the leads) of the series of Pd and Pd-Au films whose resistivity characteristics were shown in Figs. 4 and

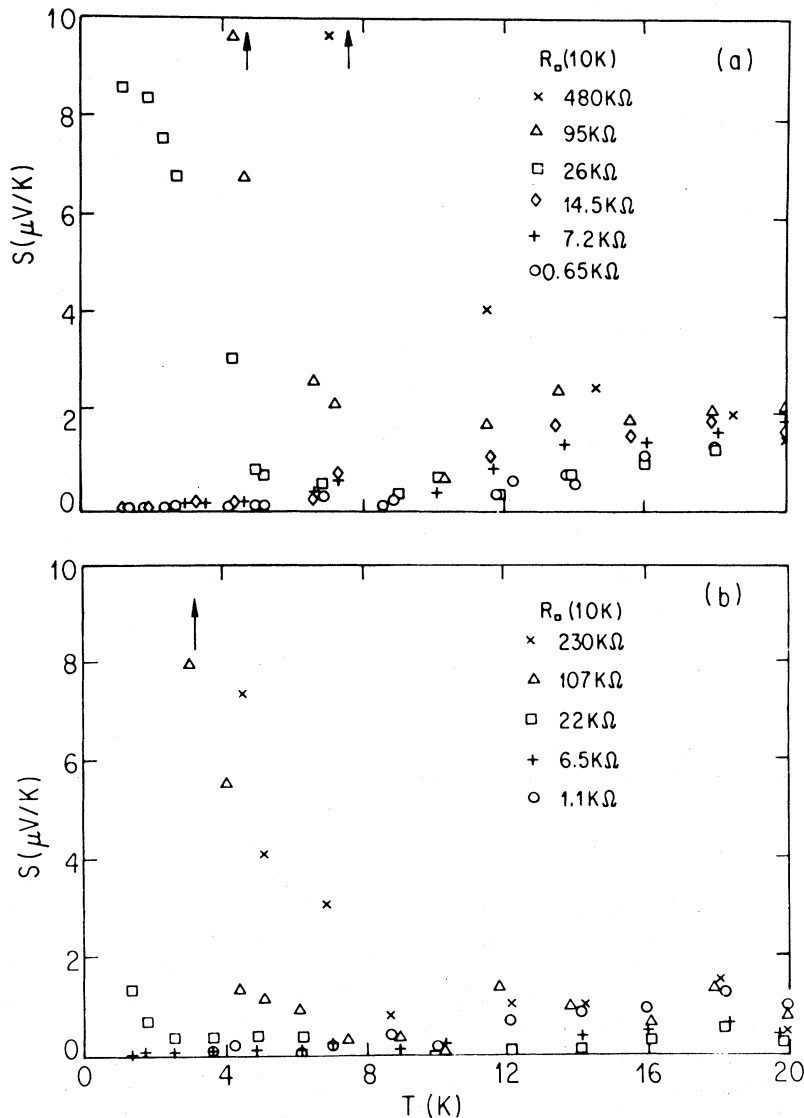


FIG. 6. Absolute thermopower as a function of temperature for (a) Pd and (b) Pd-Au films. Samples with $R_{\square} < 30$ $\text{k}\Omega/\square$ show "metallic" behavior. Samples with $R_{\square} > 30$ $\text{k}\Omega/\square$ show the presence of an energy gap.

5 is shown in Fig. 6. Figure 7 shows the thermopower of several Pd and Pd-Au films up to 100 K with resistivities above and below R_{2D} .

Above approximately 20 K the thermopowers of all the films are independent of resistivity within the accuracy of our measurements (approximately 20%) and depend only upon the material. Note in Fig. 7 that above 20 K the Pd-Au films are quite distinct from the Pd films which are similar to the published values for bulk palladium.²³

Below 20 K (Fig. 6) there is a qualitative difference between the exponential and logarithmic films. The films with $R_{\square} < R_{2D}$ follow one curve (specific

to each material) which is monotonically decreasing as temperature is lowered. The palladium film which has a resistivity of 26 $\text{k}\Omega/\square$ at 10 K and the Pd-Au film which has a resistivity of 22 $\text{k}\Omega/\square$ at 10 K follow their respective low resistance film thermopower curves and then dramatically start increasing (the Pd film at 6 K, the Pd-Au film at 3 K) as temperature is lowered, reaching values at 1.2 K which are 1–2 orders of magnitude larger than for the logarithmic films. Films of both materials with increasingly high resistance show larger low-temperature thermopowers and deviate from metallic behavior at higher temperatures.

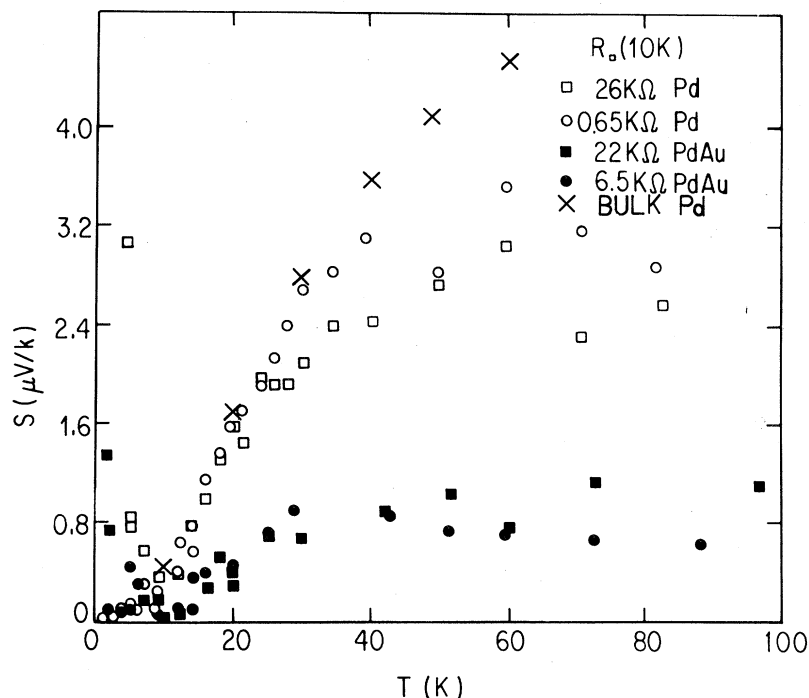


FIG. 7. Absolute thermopower as a function of temperature for each of two Pd and Pd-Au films. Notice at temperatures above 20 K the thermopower is quite material specific although independent of resistivity.

Note in Fig. 6 that the Pd sample with $R_{\square}(10\text{ K})=26\text{ k}\Omega$ has its thermopower start climbing away from the metallic films at 6 K and the Pd-Au sample with $R_{\square}(10\text{ K})=22\text{ k}\Omega$ has its start at 3 K. If one examines Fig. 5 one will see that both of these films have resistivities of approximately $30\text{ k}\Omega/\square$ at the temperature their thermopowers start deviating from metallic behavior. Note also in Fig. 6 that the Pd sample with $R_{\square}(10\text{ K})=14.5\text{ k}\Omega$ has $R_{\square}(1.3\text{ K})=20\text{ k}\Omega$ yet its thermopower is indistinguishable from the more metallic samples [such as the $R_{\square}(10\text{ K})=0.65\text{ k}\Omega$ sample] while the $R_{\square}(10\text{ K})=26\text{ k}\Omega$ sample has $R_{\square}(5\text{ K})=40\text{ k}\Omega$. We therefore suggest that the metal-insulator transition defined by the thermopower occurs close to $R_{2D}=30\text{ k}\Omega/\square$.

IV. DISCUSSION

There are two prevalent pictures of the metal-insulator transition in two dimensions which parallel the single-particle (Anderson²⁴) picture as opposed to the (Mott²⁵) Coulomb correlation picture in three-dimensional systems. In the scaling picture one goes gradually from a metal with weakly localized states that perturbatively give a logarithmic resistivity increase to an insulator with an exponen-

tial temperature dependence to the resistivity,³ while in the interacting electron picture the combined effects of the elastic scattering and the electron-electron interaction is to change the density of states in the vicinity of the Fermi energy as well as cause the logarithmic correction to the resistivity.⁴

The thermoelectric power in a Boltzmann equation treatment is often expressed in terms of a logarithmic derivative with respect to energy of a band-structure integral and a mean-free-path integral.²⁶ We expect the mean-free-path term or mobility term to be small since the dominant scattering mechanism in these films is the imperfection and boundary scattering which contributes to the elastic mean free path and the large temperature-independent part of the resistivity of the metallic samples. In the following discussion we will therefore treat the thermopower as reflecting the energy distribution of the states responsible for the conductivity.

The rigorous calculation of the thermopower is difficult even in the noninteracting picture and we will therefore be concerned mainly with its temperature dependence in the simplified derivations which follow. It is often more instructive to look at the Peltier coefficient, the coefficient which relates the heat current (dU/dt) to the electrical current (j)

which accompanies it,

$$\Pi j = dU/dt . \quad (5)$$

The thermopower can be obtained from the Peltier coefficient by an Onsager relation:

$$\Pi = ST . \quad (6)$$

For a system with a finite density of states, $N(E_F)$, at the Fermi energy the average heat per carrier is proportional to the specific heat, C , times the temperature and the heat current is CTv , with v the average electron velocity. The electrical current is $j = nev$ with n the electron density and the specific heat is $\sim nk_B[N(E_F)k_B T]$. The Peltier heat and the thermopower are then given by

$$\Pi \sim (k_B/e)[N(E_F)T]T , \quad (7a)$$

$$S = \Pi/T \sim (k_B/e)[N(E_F)T] , \quad (7b)$$

which is the usual form for the thermopower of metallic conductors. The thermopower goes to zero as the temperature decreases due to the collapse of the carrier distribution to the Fermi energy.

For insulators the characteristic heat of the carriers is the energy difference between the band edge states and the chemical potential or $\sim E_G/2$ where E_G is the energy gap. The heat current is $(E_G/2)nv$ and the thermopower is

$$S \sim (k_B/e)(E_G/2k_B T) \quad (8)$$

which illustrates the typical behavior of semiconductors at low temperature. The thermopower diverges as the carriers remain at a fixed distance from the Fermi energy as temperature is lowered.

There are several additional properties of the thermopower which are worth pointing out. The thermopower of any system with electron-hole symmetry is identically zero, so that the equations above assume that only one carrier is dominant. The third law of thermodynamics requires that the product of the thermopower times the conductivity approaches zero as $T \rightarrow 0$. Thus materials which have finite conductivity as $T \rightarrow 0$ must have vanishing thermopower. For systems with finite or diverging thermopower the conductivity must go to zero faster than $1/S$.²⁷

In the weakly localized regime ($R_{\square} \ll R_{2D}$), scaling theory suggests that transport proceeds via the accessible states within $\sim k_B T$ of the Fermi energy as is typical for a metal. The thermopower will decrease as temperature decreases and at low temperature will follow Eq. (7).¹³

Within a single-particle picture, the exponential temperature dependence of the conductivity for high resistivity samples is the result of variable range

hopping. The thermoelectric power for the case of variable range hopping is more interesting and less obvious than for the simple metal. In the brief derivation of Eq. (5) the implicit assumption was that the conducting electrons had the same energy distribution as the thermal distribution. As we shall see the "transport weighted" average energy has a different temperature dependence than simply $k_B T$ since the higher energy carriers contribute more to the conductivity in the strongly localized regime.

Following the elementary treatment of variable range hopping, the conductivity is determined by maximizing the distance that a localized electron can traverse under the opposing conditions of exponential decrease of its wave function with distance and exponential decrease of hopping probability for nearby states with large energy differences as compared to the thermal energy. For a d -dimensional system the average energy spacing between a given state and the closest energy state to it within a hypersphere of radius r is proportional to

$$\Delta E \sim 1/(dN/dE)r^d . \quad (9)$$

The probability of making a hop to a state a distance r is then reduced by e^{-ar} from the tunneling matrix elements, while it is enhanced by the factor $e^{-\Delta E/k_B T}$ from the Boltzmann statistics. According to Mott the jump rate and the conductivity are determined by maximizing the exponent of the product of these two factors. The result for the characteristic distance and the characteristic energy of a hop are then

$$r \sim (dN/dE)^{-1/d} T^{-1/(d+1)} , \quad (10a)$$

$$\Delta E \sim T^{d/(d+1)} . \quad (10b)$$

and the temperature dependence of the conductivity is

$$\sigma \sim e^{-\Delta E/T} \sim e^{-(T_0/T)^{1/(d+1)}} . \quad (11)$$

The distribution of electrons responsible for the conductivity therefore has a width of ΔE rather than $k_B T$. The expression for the Peltier heat in Eq. (5a) is then modified to

$$\Pi \sim (k_B/e)[N(E_F)\Delta E]\Delta E \quad (12)$$

and the thermopower has the form

$$S \sim (\Delta E)^2/T \sim T^{(d-1)/(d+1)} . \quad (13)$$

Thus for three dimensions the thermopower tends to zero with a square-root dependence and for the two-dimensional case of present interest it approaches zero as cube root of temperature. It is interesting to note that if variable range hopping were

ever applicable to one dimension the thermopower would be temperature independent.

This problem was first treated by Mott and Davis²⁸ for the three-dimensional case. He found $S \sim T^{1/2}$. If $d > 1$, $S \rightarrow 0$ as $T \rightarrow 0$, the thermopower decreases with decreasing temperature although the conductivity is "activated" or exponential with a fractional power of inverse temperature.

It might be expected that the presence of a disorder induced mobility gap could explain our results in a single-particle picture. However, since the samples are metallic for $R_{\square} < R_{2D}$, the Fermi energy is far from any band edges. This precludes the possibility of a mobility gap opening about the Fermi energy similar to that in a semiconductor with band tailing. The density of states is continuous and nonzero at the Fermi energy when $R_{\square} < R_{2D}$ and the thermopower reflects this by displaying metallic behavior. If a mobility gap were to open up with decreasing temperature as R_{\square} crosses above R_{2D} , the mobility edges would approach the Fermi energy rather than recede from it and if the mobility edges did reach the Fermi energy then the system would be dominated by variable range hopping.

We therefore conclude that if the single-particle localization picture is to describe the behavior of our films we should have $S \rightarrow 0$ as $T \rightarrow 0$, independent of the resistivity and its temperature dependence. This is the natural consequence of a theory which treats the metal-insulator transition entirely as a mobility effect.

In the interaction picture the combined effects of the elastic scattering and the electron-electron interaction is to change the density of states in the vicinity of the Fermi energy as well as cause the logarithmic correction to the resistivity.⁴ This change in the density of states should show up in the thermopower as a logarithmic correction to the otherwise metallic behavior¹³ of the system. The thermopower will still decrease as $T \rightarrow 0$ as long as there is a finite density of states at E_F . At present we lack the sensitivity to test this prediction. If Coulomb correlations are important then one might expect the

metal-insulator transition to occur via the reduction of the density of states at the Fermi energy until a gap opens,⁷⁻¹⁰ presumably at resistivities $\sim R_{2D}$. With the presence of a gap the thermopower takes on a characteristic semiconducting behavior with the thermopower increasing with decreasing T [$S \sim (k_B/e)E_{\text{gap}}/2k_B T$ for $E_{\text{gap}} \gg k_B T$].

The increase in the thermopower in our high-resistivity samples leads us to conclude that a gap is appearing. This favors an interpretation in terms of the interaction model. Previous tunneling measurements have also shown an interaction gap.^{11,12} We are never at sufficiently low temperature in our thermopower measurements to evaluate E_{gap} from the limiting behavior of S . However, from the temperature at which the thermopower of the high- R_{\square} samples deviates from the low- R_{\square} samples we would estimate $E_{\text{gap}}/k_B \sim 2-5$ K for the $R_{\square}(10 \text{ K}) = 26 \text{ k}\Omega$ Pd film, $E_{\text{gap}} \sim 10-20$ K for the $R_{\square} = 480 \text{ k}\Omega$ Pd film, $E_{\text{gap}} \sim 1-3$ K for the $R_{\square} \sim 22 \text{ k}\Omega$ Pd-Au film, and $E_{\text{gap}} \sim 10-20$ K for the $R_{\square} \sim 230 \text{ k}\Omega$ Pd-Au film.

V. CONCLUSION

We have found that the thermopower reflects the change in behavior between films with resistivities greater or less than $30000 \Omega/\square$ much more dramatically than does the temperature dependence of the resistivity. For low-resistivity films the thermopower shows a material specific but metallic behavior with $S \rightarrow 0$ as $T \rightarrow 0$. High-resistivity films have semiconductinglike thermopower with S increasing as T decreases indicating the opening of an energy gap. The sharpness of the transition as a function of film resistivity suggests that the gap may be opening at a well-defined value of R_{\square} and that electron-electron correlations are important.

ACKNOWLEDGMENT

This research has been supported by the National Science Foundation under Grant No. DMR-81-15241.

¹D. J. Thouless, Phys. Rep. **13C**, 93 (1974).

²D. C. Licciardello and D. J. Thouless, Phys. Rev. Lett. **35**, 1475 (1975).

³E. Abrahams, P. W. Anderson, D. C. Licciardello, and T. V. Ramakrishnan, Phys. Rev. Lett. **42**, 673 (1979).

⁴Patrick A. Lee, Phys. Rev. Lett. **42**, 1492 (1979).

⁵B. L. Altshuler, D. Khmel'nitzkii, A. I. Larkin, and P. A. Lee, Phys. Rev. B **22**, 5142 (1980).

⁶B. L. Altshuler, A. G. Arnov, and P. A. Lee, Phys. Rev.

Lett. **44**, 1288 (1980).

⁷A. L. Efros and B. I. Shklor'skii, J. Phys. C **8**, L49 (1975).

⁸A. L. Efros, J. Phys. C **9**, 2021 (1976).

⁹A. L. Efros, N. VanLien, and B. I. Shklor'skii, Solid State Commun. **32**, 851 (1979).

¹⁰B. Abeles, in *Applied Solid State Science*, edited by R. Wolfe (Academic, New York, 1976), Vol. 6, p. 1.

¹¹R. C. Dynes and J. P. Garno, Phys. Rev. Lett. **46**, 371 (1981).

- ¹²W. L. McMillan and J. M. Mochel, Phys. Rev. Lett. **46**, 556 (1981).
- ¹³C. S. Ting, A. Houghton, and J. R. Senna, Surf. Sci. **113**, 244 (1982); Phys. Rev. B **25**, 1439 (1982).
- ¹⁴R. C. Dynes, J. P. Garno, and J. M. Rowell, Phys. Rev. Lett. **40**, 479 (1978).
- ¹⁵G. J. Dolan and D. D. Osheroff, Phys. Rev. Lett. **43**, 721 (1979).
- ¹⁶D. J. Bishop, D. C. Tsui, and R. C. Dynes, Phys. Rev. Lett. **46**, 360 (1981); **44**, 1153 (1980).
- ¹⁷L. Van den Dries, C. Van Haesendonck, Y. Bruynseraede, and G. Deutscher, Phys. Rev. Lett. **46**, 565 (1981).
- ¹⁸D. A. Poole, M. Pepper, and R. W. Glew, J. Phys. C **14**, L995 (1981).
- ¹⁹W. C. McGinnis, M. J. Burns, R. W. Simon, G. Deutscher, and P. M. Chaikin, Physica B + C **107**, 5 (1981).
- ²⁰M. J. Burns, W. C. McGinnis, R. W. Simon, G. Deutscher, and P. M. Chaikin, Phys. Rev. Lett. **47**, 1620 (1981).
- ²¹W. C. McGinnis and P. M. Chaikin (unpublished).
- ²²A. F. Ioffe and A. R. Regel, Prog. Semicond. **4**, 237 (1960).
- ²³F. J. Blatt, P. A. Schroeder, C. L. Foiles, and D. Greig, *Thermoelectric Power of Metals* (Plenum, New York, 1976).
- ²⁴P. W. Anderson, Phys. Rev. **109**, 1492 (1958).
- ²⁵N. F. Mott, *Metal Insulator Transitions* (Taylor and Francis, London, 1974).
- ²⁶J. M. Ziman, *Electrons and Phonons* (Clarendon, Oxford, 1960).
- ²⁷J. Tauc, *Photo and Thermoelectric Effects in Semiconductors* (Pergamon, New York, 1962).
- ²⁸N. F. Mott and E. A. Davis, *Electronic Processes in Non-Crystalline Materials* (Clarendon, Oxford, 1979), p. 55.

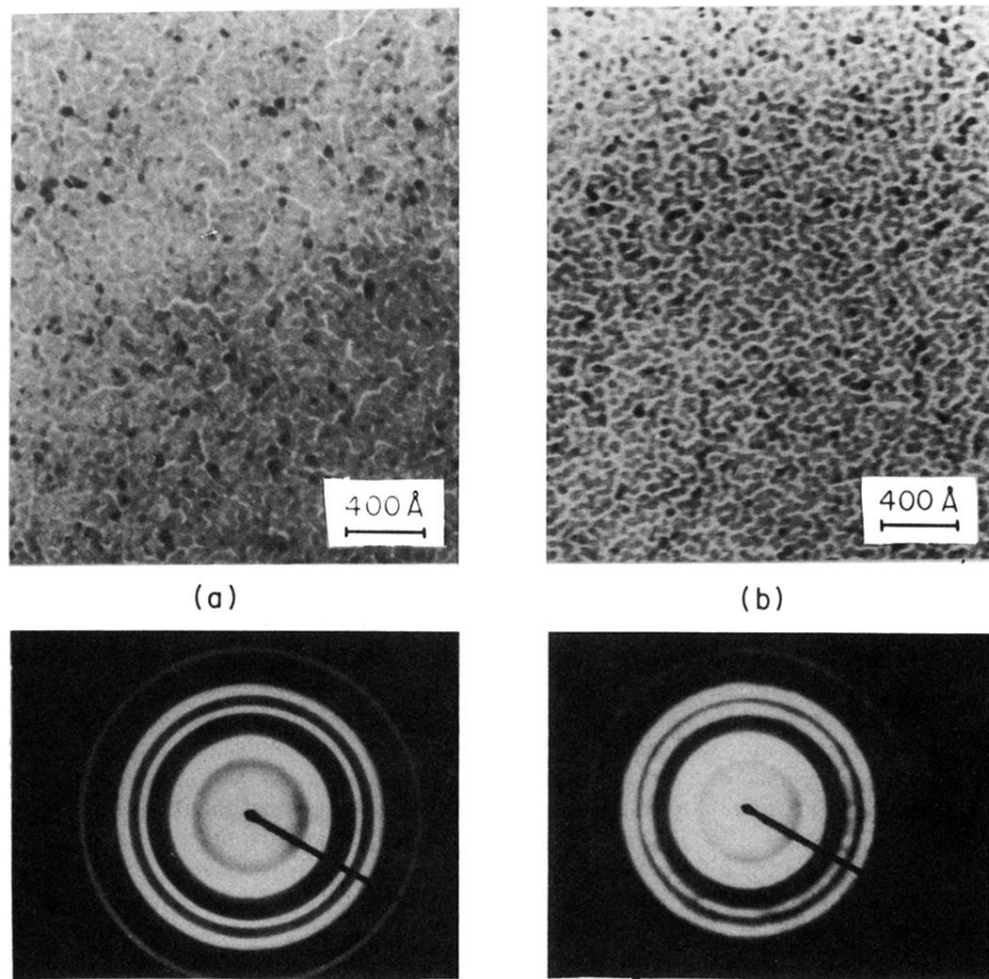


FIG. 1. Electron micrograph and electron diffraction pattern of (a) nominal 24-Å-thick palladium film, (b) nominal 25-Å-thick palladium-gold film. Both films are deposited on carbon-coated grids.